

## Development of a simulation-based process chain: strategy for different levels of detail for the preprocessing definitions

Toni A. Krol, Sebastian Westhäuser, M. F. Zäh, Johannes Schilp, G. Groth

### Angaben zur Veröffentlichung / Publication details:

Krol, Toni A., Sebastian Westhäuser, M. F. Zäh, Johannes Schilp, and G. Groth. 2011.  
"Development of a simulation-based process chain: strategy for different levels of detail  
for the preprocessing definitions." *SNE Simulation Notes Europe* 21 (3-4): 135–40.  
<https://doi.org/10.11128/sne.21.tn.10081>.

### Nutzungsbedingungen / Terms of use:

licgercopyright

Dieses Dokument wird unter folgenden Bedingungen zur Verfügung gestellt: / This document is made available under these conditions:

#### Deutsches Urheberrecht

Weitere Informationen finden Sie unter: / For more information see:

<https://www.uni-augsburg.de/de/organisation/bibliothek/publizieren-zitieren-archivieren/publiz/>



# Development of a Simulation-Based Process Chain – Strategy for Different Levels of Detail for the Preprocessing Definitions

Toni A. Krol<sup>1\*</sup>, Sebastian Westhäuser<sup>1</sup>, M. F. Zäh<sup>1</sup>, Johannes Schilp<sup>1</sup>, G. Groth<sup>2</sup>

<sup>1</sup>iwb Anwenderzentrum, Technische Universität München, Beim Glaspalast 5, 86153 Augsburg, Germany

<sup>2</sup>CADFEM GmbH, Grafting / Munich; \*[Toni.Krol@iwb.tum.de](mailto:Toni.Krol@iwb.tum.de)

**Abstract.** Additive manufacturing processes fulfill the actual market demands with regard to a high individuality and complexity of products. Hence, these processes are used nowadays in different branches (e. g. aerospace, automotive, medical industry). Further-more, a high process stability and reproducibility is requested by the user for an eco-nomic application of this technology. Up to now, these targets are reached by numerous test rigs on the manufacturing system which causes high resource consumption.

For increasing the efficiency of metal-based additive manufacturing (AM), the employees of the iw b application center Augsburg in corporation with the CADFEM GmbH and four further partners develops a simulation-based process chain (founded by the Bavarian Research Foundation). Before the production process is started, an analysis of the structural part behavior as well as a process optimization should be performed using the finite element analysis (FEA). Due to the complexity of the thermal-ly activated process, it is necessary to select the appropriate FE-modeling strategy for enhancing the target figures calculation efficiency and accuracy. Hence, in this work a strategy will be presented, which can map different levels of detail for the preprocess-ing definitions. These local and global descriptions can be realized by using suitable contact definitions (contact elements) to link different element meshes. Additionally, the user can select different layers of the part geometry, which should be analyzed in detail within the simulation. Also layer-specific distortions and residual stresses can be calculated while saving calculation time. Furthermore, with this approach the process history and therefore the whole part geometry can be considered in the structural calculations. A validation of the transient temperature field and the mechanical part properties is presented by the comparison with measured values.

## Introduction

Companies remain competitive in the future, if they manufacture industrial goods in shorter production cycles [1]. Hence, the customer demands regarding the production systems are changing. Prospectively, the use of production technologies that assure an economic production of parts in small quantities is important. Metal-based, additive processes, which are presented in this work, comply with the named requirements.

Based on a powder coat (different metals can be used), the part is solidified in single layers with a beam source (laser- or electron-beam). The layers are created directly from the CAD-Model, while using different interface formats. With lowering the building platform, the application of a new powder layer and the solidification process, the part is build up sequentially in the manufacturing system [2]. Further-more, the thermally activated, additive process causes high temperature gradients in the manufactured part. These gradients depend on the used exposure and coating time. The process-related temperature gradient mechanism (TGM) is causing distortions and residual stresses in the produced part. Hence, with an incorrect dimensioning of the production process, due to an incorrect choice of process parameters, the structural part properties can induce defects (eruptions, delamination) as well as direct failures during the manufacturing process (cp. error patterns in Figure 1).

Hence, for realizing a production without defective products, high process knowledge is demanded from the operator (cf. [3]). To achieve a stable and repeatable production, the application of digital tools (e. g. simulation) is of great significance for the economization of resources.

## 1 Simulation Models for Powder Coated Additive Processes

Different institutions and researchers work on the simulation of metal-based, additive manufacturing using the finite element analysis (FEA). Thereby, it can be distinguished between process-, material- and structural-simulation (cf. [4]). All three simulation disciplines exhibit different detail levels with regard to the process mapping and calculation of additive processes. Using the process simulation, the heat affected zone and thus the beam-material interactions can be mapped in detail.

For example [5] developed heat source models for additive manufacturing, to analyze the heat transfer during the application of the heat load. Furthermore, they examined the impact of a high beam source velocity on the stability of the welding seam within their simulation model. A similar investigation performs [6]. With the definition of equivalent heat source models in the simulation he analyzed the effect of the scanning velocity and beam power on the thermal part behavior.

Concerning the structural simulation, [4] and [7] developed technology-specific simulation systems for providing adapted simulation models to different user groups. Hence, single layers and layer-specific data are mapped within the developed layer-based model, whereas the calculation of the whole part geometry is realizable with using reduction strategies (summarization of layers, abstraction of scanning strategies) within the global-based model.

[14] present the demand of considering the material behavior in the structural simulation. [8] and [9] use temperature-dependent material models. Furthermore, [10] maps the powder coat in the simulation model with using a continuous medium theory and a local, isotropic and homogenous material behavior. The presented works demonstrate the need for an interdisciplinary connection between the simulation disciplines (structure, process and material) for a realistic mapping of metal-based, additive processes.

Hence, not only the used detail level has to be considered while applying loads and boundary conditions. On the contrary, this includes also the definition of the FE-geometry in the preprocessing of the simulation system.

Thus, [10] uses an element division which depends on the resulting temperature gradients.

This approach allows a refined meshing of the heat effected zone with cubic elements ( $10\ \mu\text{m} \times 10\ \mu\text{m} \times 20\ \mu\text{m}$ ) and hence the application of a detailed heat source. Further FE-geometry elements are meshed with using an element size of  $100\ \mu\text{m} \times 100\ \mu\text{m} \times 100\ \mu\text{m}$ . In contrast [7] and [11] use different net shapes for different simulation models. While the global-based model exhibit an element size of  $500\ \mu\text{m} \times 500\ \mu\text{m} \times 500\ \mu\text{m}$ ,  $100\ \mu\text{m} \times 100\ \mu\text{m} \times 20\ \mu\text{m}$  elements are applied for the detail-based model.

These works are mostly regarding a static arrangement of the elements or are only usable within one layer. Furthermore, only model dependent process parameters can be analyzed. Due to the complexity of the production process, only layer specific process settings for single layers (cf. [12]), or layer overlapping parameters using reduction strategies can be confronted and rated (cf. [13]) at the same time.

## 2 Method-system for Creating User-specific Simulation Models

Metal-based, additive manufacturing processes require a variety of calculation steps with a detailed mapping of this technology by means of the finite element analysis. As mentioned in chapter 2, [7] enables the mapping of technology specific simulation models with using reduction strategies for an efficient calculation of the whole part as well as the detailed mapping of single layers. The received results are the initial basis for this work. However, for a simulation-based optimization of metal-based, additive manufacturing the advantages of a layered, dynamic adaption of the FE-geometry and the process boundary conditions should be used and summarized in a new research approach.

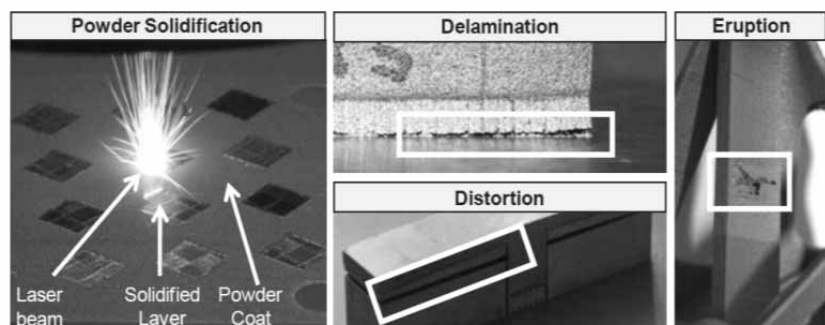


Figure 1: Powder solidification and typical error patterns of layered manufacturing.

By means of an abstract process model the calculation of the transient temperature field and thermo-mechanical values (residual stresses and distortions) should be performed with the option to detail every single layer in the mapping accuracy. This allows a layer-specific comparison of calculated dimensions. Furthermore, the user can choose between different detail and abstraction levels in future. This includes different modeling types for the scanning strategy, the support modeling and the merging of layers (cp. Figure 2).

Regarding the scanning strategy the heat flux during the solidification phase can be applied on single beam source vectors (so called hatches), using a distributed scanning pattern on single segments, or on the whole layer. The dimension of the process abstraction increases in this order. The unconsidered heat load distribution within a single layer should be regarded, when using a layer-specific exposure. By means of a twin-cantilever-structure (t-profile) with layer dimensions of 70 mm x 10 mm [11] verified the plausibility of this approach by comparing measured and simulated values. However, operators of additive manufacturing systems use distributed scanning strategies nowadays (cp. Figure 2).

Thus, scanning vectors can be summarized to layer segments and are therefore suitable for a simultaneous application of the heat flux. Compared to a layer-specific exposure, this approach increases the calculation accuracy. Supports are used in the process for transporting heat from the above solidified layers and are supporting protruding part areas during manufacturing. Because these structures are not enhancing the appreciation of the product, these structures are mostly filigree and are consisting of single grid structures (cp. Figure 2).

Hence, the width of a solidified support bridge complies with the diameter of the beam source (LBB in Figure 2). A construction of an element mesh with 2½-D shell elements with 4 nodes is therefore sufficient. However, if mapping sheet metals as product geometry, the supports can exhibit a high degree of the total solidified vol-

ume. A detailed modeling of these structures is linked with a higher calculation effort. [7] analyzed the possibility of a continuum-mechanic mapping of supports in the structural simulation. This approach includes controlling the structural behavior of supports with the definition of orthotropic material properties.

Thus, factors that are calculated from the geometrical dimensions of support structures are multiplied with thermal (density, thermal conductivity) and thermo-mechanical (young's modulus, shear modulus) values of the solid material. [14] enhanced this approach, to regard further support geometries (e. g. with a web- or line pattern) (cp.  $f_{sgx,y}$  in Figure 2). Thereby, the factors are calculated layer-specific, whereas the layer geometry is considered in the material adjustments for the support. The limit of this modeling type represents the support gapping. With increasing LGD the Young's modulus decreases. This effect should be regarded if modeling a bilinear kinematic hardening. Small values for the Young's modulus can cause calculation convergence problems, when applying high temperature loads.

Nowadays additive manufactured parts can be produced with a height of 300 mm. 10,000 layers have to be solidified if the whole height and a layer thickness of 30 µm is used. It is not feasible to analyze all layers in detail due to the actual available computer architecture.

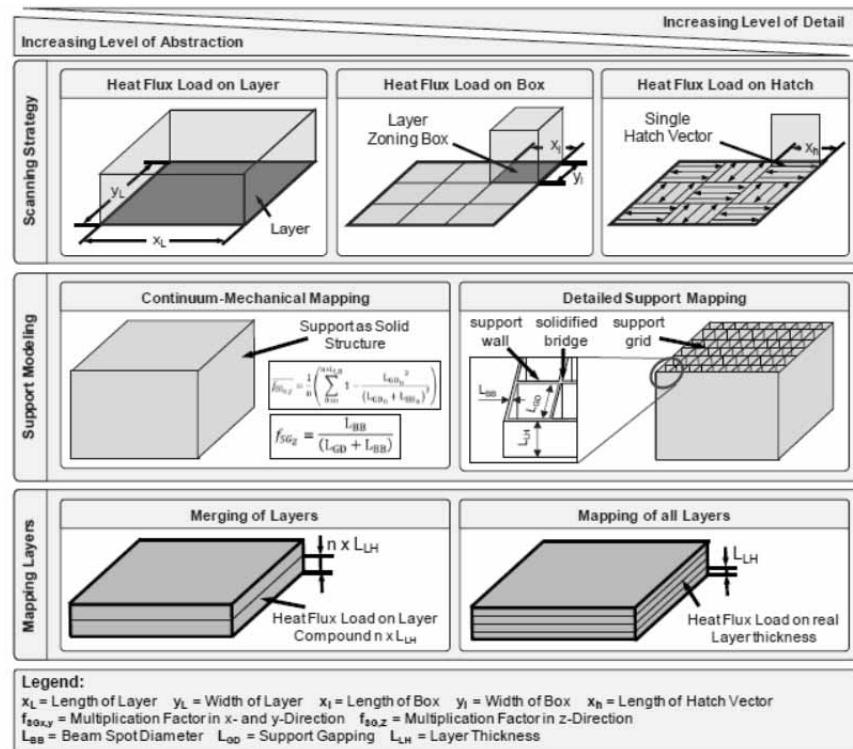


Figure 2: Modeling types for the structural simulation of layered manufacturing

This will cause enormous calculation times, especially if different process parameter adjustments are compared. Hence, merging of layers to layer compounds should be mapped within the element pattern and should be applied with a common heat source. The validation of this approach proofed also [11]. However, with large layer dimensions and a low amount of layers, the mapping of all layers is expedient.

The choice of the presented modeling types is dependent on the customer demands. The selection should be determined according to the product geometry and the analyzed target figure. In future, the combination of the modeling types visualized in Figure 2 should be possible. Furthermore, the user can change the abstraction and detail levels before solving the simulation problem. Single layers can be analyzed more in detail regarding the structural part's characteristics, whereas the remaining FE-geometry is calculated with a higher abstraction level.

The differences in the mesh topology can be equalized by different methods of mesh linking. Compared with the option "constraint equations" that should be applied on the surfaces of the layer meshes that have to be interconnected, contact element definitions allow a higher range of adjustment possibilities. The functionality of a dynamic detailing model is therefore demonstrated in the following by means of an application scenario.

### 3 Application of the Method - System for a Dynamic Detail Level

[11] and [15] used twin-cantilever structures for analyzing the structural part's characteristics. For establishing the same knowledge base and for the comparableness of the results, the geometry shape is taken as a basis for this research work. Due to the symmetry of this part, only one wing area is considered (cp. Figure 3). This allows a fast measurement value logging (cp. chapter 4) and the efficient solving of the simulation problem.

Following the abstraction and detail levels presented in Figure 2, two different modeling types were combined with contact definitions. The lowest layer of the wing area is representing a detailed process mapping, which allows also a particular support construction. Due to the distributed scanning pattern in this area, according to the specifications of the man-

ufacturing system control, a finer mesh of the geometry with  $0,1 \times 0,1 \times 0,2 \text{ mm}^3$  is realized (cp. preprocessing definitions Figure 4).

The remaining layers are provided with a higher abstraction concerning the scanning strategy, the merging of layers to layer compounds and the continuum-mechanical mapping of supports. For a significant improvement of the calculation efficiency a mesh with  $2 \times 2 \times 0,5 \text{ mm}^3$  is used. Hence, these two mesh topologies are joined with using contact elements (cf. Figure 3). As shown in Figure 4, "Surface-to-Surface" contact definitions are applied between the part models.

The support in the detailed process mapping is modeled with shell elements. Due to the corresponding geometry configuration "Node-to-Surface" contacts are used for joining the support areas. The detailed layer is positioned between layers of the abstract process mapping. Hence, a contact pair (consisting of contact and target elements) is defined on the bottom and top of the detailed layer (cp. Figure 3). The needed contact force for fulfilling the contact conditions can be calculated by multiplying the resulting stiffness with the contact penetration subtracted from the reverse acting, applied load (cf. [16]).

As shown in Figure 4, an exemplarily contact definition for the layer  $n+1$  is performed to detail the mesh topology. On the basis of the thermal material data (cp. Figure 4) as well as the deposited layering gathered from the preprocessing definitions, the calculation of the transient temperature field can be performed. [17] and [18] describe therefore the thermal equilibrium equation. Additionally, the definitions of the contact junction can be adjusted with "keyoptions" of the corresponding elements. Hence, the amount of degrees of freedoms is set to temperature calculations. Because of the direct abutment of the contacts to volume or shell elements, only a heat transfer should be modeled. The corresponding thermal contact conduction is defined with (cf. [17] and [16]):

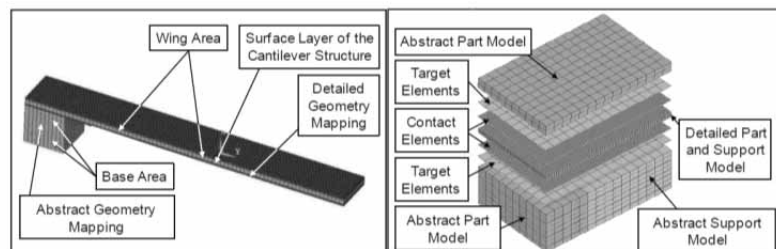


Figure 3: Cantilever structure and schematic sketch of coupling different detail levels.

$$\frac{\delta Q}{\delta \alpha} = K_c \left( \frac{\delta T_r}{\delta \alpha} - \frac{\delta T_c}{\delta \alpha} \right) \quad (1)$$

In this equation  $Q$  is defined through the heat flux that is calculated by the thermal equilibrium equation  $K_c$ , describes the thermal contact conductance coefficient  $T_r$  is the resulting temperature at the target surface and  $T_c$  is the temperature at the contact surface.

In the mechanical analysis the temperatures as well as the assignment to nodes and times are the basis for these calculations. Regarding the used material data (temperature dependent stress-strain-relations, thermal dilatation and contraction) the structural part properties are solved by the dynamic transient equilibrium equation (cf. [18], [14] and [17]).

For the corresponding contact definition the “Augmented Lagrangian Method” is used (cf. [16]), after changing the degrees of freedom to distortions. The needed pressure for closing the contact is defined by following equation (cf. [17]):

$$P = \begin{cases} 0 & \text{if } u_n > 0 \\ K_n \times u_n + \lambda_{i+1} & \text{if } u_n \leq 0 \end{cases} \quad (2)$$

$K_n$  describes the contact normal stiffness,  $u_n$  is the contact gap size and  $\lambda_{i+1}$  is defined by following correlation (cf. [17]):

$$\lambda_{i+1} = \begin{cases} \lambda_i + K_n \times u_n & \text{if } |u_n| > \varepsilon \\ \lambda_i & \text{if } |u_n| < \varepsilon \end{cases} \quad (3)$$

Hence,  $\lambda_i$  is the Lagrange multiplier component at iteration  $i$  and  $\varepsilon$  is the compatibility tolerance. Furthermore, with adjusting the contact “keyoptions” an adjustment of the contact status to “always bonded” is realized. That means, that the equation for  $u_n \leq 0$  corresponds to  $u_n > 0$ . Due to the resulting layer compound in the manufacturing process this adjustment should be considered as useful.

## 4 Calculation and Measurement of the Transient Temperature Field

For verifying the modeling approach presented in Chapter 3, the comparison of calculated results with measured values is performed by recording thermal data from a thermal imaging camera. The transient temperature field is captured during the manufacturing of the cantilever (cp. Figure 3). Different from the simulation model, the abstraction levels are not active in production. Thus, the part generation in the manufacturing system corresponds to a detailed modeling in the simulation (cp. Figure 2).

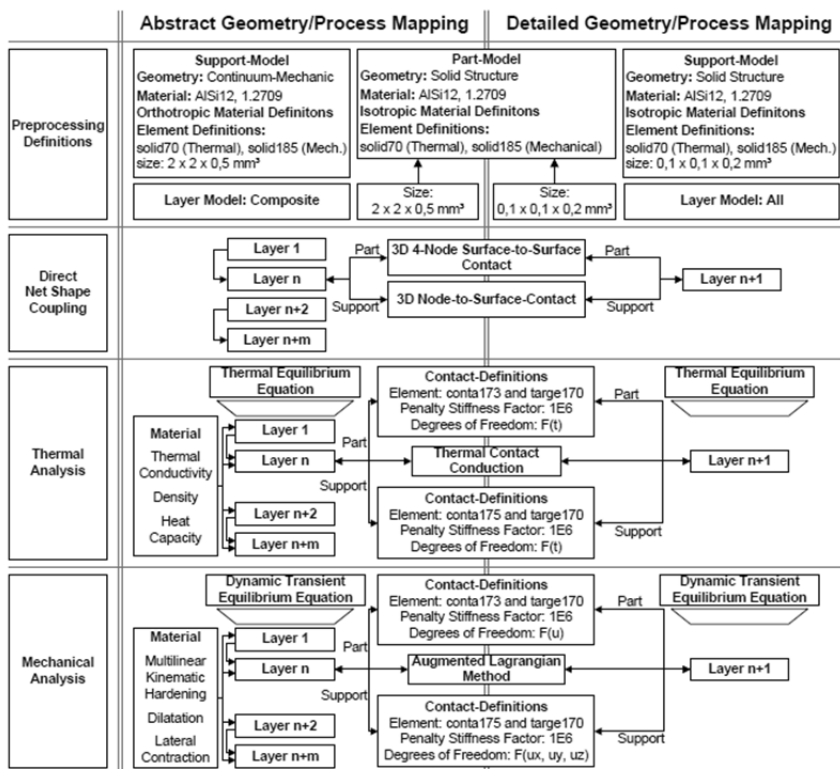
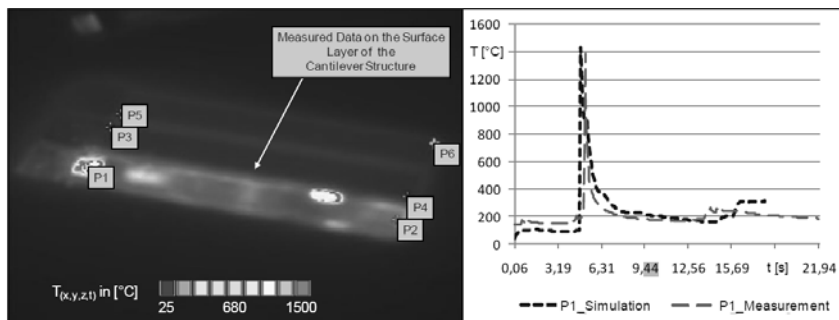


Figure 4. Procedure for the application of a dynamic model detailing.

This comparison allows proofing the validity of the used abstraction methods. Furthermore, the detailed layer in the simulation was also used for the measurements (cp. Figure 4). In the measurement field different measuring points named from P1 to P6 were de-fined. These correspond to the positions in the extracted simulation results. Figure 5 is displaying the temperature distribution and the graphs of the temperature profile at measurement point P1.

The curve shapes exhibit that the time course while applying heat loads are matching approximately. There is a peak recognizable at 5 s that is caused by the heat flux of the distributed scanning pattern. At this point of time the beam source (heat load) is directly at measuring point P1.



**Figure 5.** Comparison of the transient temperature profile using a cantilever structure.

The next local temperature increase between 13 s and 16 s indicate an exposure of a neighboring powder area relatively to the measuring point. The time offset between measurement and simulation at this point is caused by the element divisions. The heat load application can be performed more precisely if re-fining the element size, whereas the calculation time increases drastically. The offset of temperatures between both curves from 0 s to 5 s is caused by using a partially transparent germanium glass in front of the thermal imaging camera for the needed separation of the process from the environment. Nevertheless, with controlling the emission coefficient during the interpretation of the measured values a better alignment could not be reached.

## 5 Summary and Future Perspectives

Using metal-based additive manufacturing processes the operator is able to manufacture efficiently complex and individual parts. As shown in chapter 2, distortions and residual stresses are a result of the thermal activated process. The simulation based on the finite element analysis allows the optimization of the process before the production is started. This work presents a method for the dynamic coupling of different detail and abstraction levels in order to create the simulation model (cp. chapter 3).

Using this method the whole part as well as the distributed scanning pattern can be mapped with one simulation model. As shown by the application of the method with a benchmark geometry in chapter 4, the detail level can be increased in every single layer employing contact elements.

Hence, the user can choose between the presented modeling options in Figure 2. The results of the theoretical examination are verified by the comparison of the transient temperature field between simulation and calculation in chapter 5.

Further investigations with regard to the application of abstract process mapping should be performed using different product geometries to analyze the global applicability of the

methods. Furthermore, a comparison between measured and simulated results concerning the structural part behavior should be conducted. Therefore, measurements with neutron diffractometry (for measuring residual stresses) and optical measurement systems (for measuring distortions) are necessary.

## References

- [1] M. F. Zaeh. *Wirtschaftliche Fertigung mit Rapid-Technologien. Anwender-Leitfaden zur Auswahl geeigneter Verfahren.* iwv Anwenderzentrum Augsburg, TU Muenchen. Muenchen. Germany, Hanser 2006. ISBN: 9783446228542.
- [2] A. Gebhardt. *Generative Fertigungsverfahren. Rapid Prototyping, Rapid Tooling, Rapid Manufacturing.* 3. Aufl. Muenchen, Germany: Hanser 2007. ISBN 9783446226661.
- [3] M. van Elsen. *Complexity of selective laser melting.* Ph.D. Thesis. Katholieke Universiteit Leuven 2007.
- [4] M. F. Zaeh, G. Branner, T. A. Krol. *A three dimensional FE-model for the investigation of transient physical effects in Selective Laser Melting.* In: Bártolo, J. P. (Hrsg.): *Innovative Developments in Design and Manufacturing - Advanced Research in Virtual and Rapid Prototyping (Proceedings of VR@P4).* London: Taylor & Francis 2009. ISBN: 978-0-415-87307-9.
- [5] A. V. Gusarov, I. Yadroitsev, P. Bertrand, I. Smurov. *Model of Radiation and Heat Transfer in Laser-Powder Interaction Zone at Selective Laser Melting.* Journal of Heat Transfer 131 (July 2009) 7, pp. 072101-1 - 072101-10.

Accepted ASIM SST Winterthur, September 2011

Submitted: September 2011

Accepted November 30, 2011